Disease-related amyloidogenic variants of human lysozyme trigger the unfolded protein response and disturb eye development in *Drosophila melanogaster*

Janet R. Kumita,[*,1] Linda Helmfors,[§,1] Jocy Williams,[†] Leila M. Luheshi,[*] Linda Menzer,[‖] Mireille Dumoulin,[‖] David A. Lomas,[¶] Damian C. Crowther,[‡,¶] Christopher M. Dobson,[*] and Ann-Christin Brorsson[§,2]

*Department of Chemistry, †Department of Biochemistry, and ‡Department of Genetics, University of Cambridge, Cambridge, UK; §Division of Molecular Biotechnology, Department of Physics, Chemistry and Biology, Linköping University, Linköping, Sweden; ‖Laboratory of Enzymology and Protein Folding, Centre of Protein Engineering, Institute of Chemistry B6c, University of Liège, Liège, Belgium; and ¶Cambridge Institute for Medical Research, Cambridge, UK

ABSTRACT We have created a *Drosophila* model of lysozyme amyloidosis to investigate the *in vivo* behavior of disease-associated variants. To achieve this objective, wild-type (WT) protein and the amyloidogenic variants F57I and D67H were expressed in *Drosophila melanogaster* using the *UAS-gal4* system and both the ubiquitous and retinal expression drivers *Act5C-gal4* and *gmr-gal4*. The nontransgenic w^{1118} *Drosophila* line was used as a control throughout. We utilized ELISA experiments to probe lysozyme protein levels, scanning electron microscopy for eye phenotype classification, and immunohistochemistry to detect the unfolded protein response (UPR) activation. We observed that expressing the destabilized F57I and D67H lysozymes triggers UPR activation, resulting in degradation of these variants, whereas the WT lysozyme is secreted into the fly hemolymph. Indeed, the level of WT was up to 17 times more abundant than the variant proteins. In addition, the F57I variant gave rise to a significant disruption of the eye development, and this correlated to pronounced UPR activation. These results support the concept that the onset of familial amyloid disease is linked to an inability of the UPR to degrade completely the amyloidogenic lysozymes prior to secretion, resulting in secretion of these destabilized variants, thereby leading to deposition and associated organ damage.— Kumita, J. R., Helmfors, L., Williams, J., Luheshi, L. M., Menzer, L., Dumoulin, M., Lomas, D. A., Crowther, D. C., Dobson, C. M., Brorsson, A.-C. Disease-related amyloidogenic variants of human lysozyme trigger the unfolded protein response and disturb eye development in *Drosophila melanogaster*. FASEB J. 26, 000–000 (2012). www.fasebj.org

HUMAN LYSOZYME IS A 14-kDa globular protein that plays a role in innate immunity by catalyzing the hydrolysis of the peptidoglycan components of bacterial cell walls (1). Concordant with this role, the protein is abundant in secretions such as tears and saliva, but in the early 1990s, two naturally occurring mutational variants, the I56T and D67H lysozymes, were found to result in abnormal deposition of aggregated protein in organs such as the liver, spleen, and kidney (1, 2). Such accumulation of protein aggregates is thought to be the primary cause of dysfunction in these organs and the resulting syndrome of familial systemic amyloidosis (2, 3). Other lysozyme variants have now been found to be associated with amyloidosis, including two other single point mutations (F57I, W64R) and two double mutations (F57I/T70N, T70N/W112R) (4–6).

The folding mechanism of lysozyme has been studied in great detail (7–18), and it is clear that deposition of the lysozyme variants is a consequence of the local and transient unfolding of the protein that results in a high propensity for the protein to aggregate and form threadlike structures known as amyloid fibrils. Experimental studies of the misfolding and aggregation behavior of lysozyme *in vitro* have revealed that fibril formation occurs because the native state of lysozyme is destabilized in the amyloidogenic variants, resulting in a decreased difference in the energy barrier between the native state and partially unfolded intermediates for these variants relative to the wild-type (WT) protein (10). As a result, the amyloidogenic variants have a significantly higher ability, relative to the WT protein, to populate partially unfolded transient intermediate species, which leads to the formation of aberrant inter-

molecular interactions that result in aggregation and ultimately fibril formation (3, 13, 17, 19–26).

In contrast to the wealth of information about folding and misfolding processes of the variant lysozymes *in vitro*, much less is known about how they fold, misfold, and aggregate *in vivo*. Two interesting observations are that deposits formed in heterozygotic patients with lysozyme amyloidosis are composed entirely of the variant proteins (3) and, at least for W64R, that the circulating levels of the lysozyme variant in patients appear to be greatly reduced (4). Similarly, low levels of secretion for the amyloidogenic variant lysozymes have been observed in studies in which the proteins were expressed in the yeast *Pichia pastoris*. In this system, a direct correlation was found between the secreted quantity of any given lysozyme variant and the measured stability of its corresponding native state (27). Thus, the quality control mechanisms in yeast are able to recognize destabilized variants of lysozyme and target them for degradation. Indeed, recent studies have identified that the expression of the amyloidogenic lysozyme variant I56T in *P. pastoris* results in the up-regulation of genes related to the unfolded protein response (UPR), endoplasmic reticulum (ER)-associated degradation (ERAD), and ER-phagy processes, whereas the WT protein elicits no significant response (28).

The presence of misfolded proteins in the ER causes stress and induces the UPR, whose role is to restore ER homeostasis. One way in which this situation can be achieved is by degrading the accumulated misfolded proteins through ERAD, which is the likely fate of a substantial population of the destabilized lysozyme variants. In addition, the UPR also maintains ER homeostasis by decreasing the rate of transcription and translation, up-regulating the expression of genes that relate to proteins that assist in correct folding processes, and expanding the size and capacity of the ER. However, if homeostasis cannot be achieved and the UPR is sustained, the result can be the triggering of cell death (29).

One approach to understanding protein misfolding diseases in greater detail is to make use of model organisms such as *Drosophila melanogaster*, which can facilitate the investigation of the biological events associated with the controlled introduction of peptides or proteins prone to misfold and to aggregate *in vivo*. This method has proved to be of great relevance in studies of Alzheimer's disease in which the amyloid β-peptide (Aβ) has been expressed (30–32), for polyglutamine-repeat disorders, such as Huntington's disease (33–35), and for a familial amyloidotic polyneuropathy associated with mutational variants of transthyretin (36, 37). To study the *in vivo* behavior of variant lysozymes, we have overexpressed the WT protein, the destabilized non-natural I59T variant, and the amyloidogenic variants F57I and D67H in different tissues of *D. melanogaster*.

MATERIALS AND METHODS

All restriction enzymes were purchased from New England Biolabs (Hitchin, UK), PfuTurbo DNA polymerase from Stratagene Europe (Amsterdam, the Netherlands), and synthetic oligonucleotides from Operon (Cologne, Germany), and all chemicals were purchased from Sigma-Aldrich (Gillingham, UK) unless otherwise stated.

Generation of transgenic lysozyme flies

The genes for WT and D67H lysozyme were fused to the 3′ end of the coding DNA for an insect secretion signal peptide, MASKVSILLLLTVHLLAAQTFAQ (38), by PCR amplification that introduced unique *Eco*RI and *Not*I sites at the 5′ and 3′ ends of the coding sequence, respectively. These sites were used to clone the constructs into the *gal4*-responsive pUAST expression vector to generate UAS-lysozyme transgenes for pseudorandom incorporation into the genome of *D. melanogaster*. The constructs obtained for WT, F57I, I59T, and D67H lysozymes were then subcloned using the same sites into the *pBS-LoxP-white-Lox2272* expression vector (a gift from Prof. Stephen Small, Department of Biology, New York University, New York, NY, USA), which allows for Cre-mediated recombination for targeted transgenesis in *Drosophila* (39). The *pBS-LoxP-white-Lox2272* expression vectors containing the gene encoding WT, F57I, I59T, or D67H were injected by BestGene Inc. (Chino Hills, CA, USA), using a *Drosophila* line that has a chromosome 2 target site.

qRT-PCR analysis

Several lines of pUAST-transgenic flies were created for WT and D67H lysozyme constructs. Two lines of each (WT[a], WT[b], D67H[c], and D67H[d]) were selected, and male flies (including negative control *w[1118]* flies, which do not express human lysozyme) were crossed with *Act5C-gal4* virgins. Twenty male offspring were collected on the day of eclosion, and RNA was extracted using the Qiagen RNeasy Mini kit and treated with RNase-Free DNase (Qiagen Ltd., Crawley, UK) according to the manufacturer's protocol for purification of total RNA from animal tissues. The concentration of total RNA purified for each line was measured using a NanoDrop 1000 spectrophotometer (Thermo Fisher Scientific, Loughborough, UK), and 1 μg RNA was then subjected to reverse transcription using the Promega Reverse Transcription System with oligo dT primers (Promega, Southampton, UK). qRT-PCR was performed using a Bio-Rad iCycler and 2X iQ SYBR Green Supermix (Bio-Rad Laboratories, Hemel Hempstead, UK). Each sample was analyzed in triplicate with both the target gene (lysozyme) and the control gene (*RP49*) primers in parallel. The primer sequences for the lysozyme gene were sense, 5′-CCAACTACAACGCTGGTGAC-3′, and antisense, 5′-CTGCAGCAAAGCAGAACAAG-3′; those for the *RP49* gene were sense, 5′-ATGACCATCCGCCCAGCATCAGG-3′, and antisense, 5′-ATCTCGCCGCAGTAAACG-3′. Relative expression levels were calculated using the Livak method (40).

Immunohistochemistry of larvae

WT[b], D67H[c], and control *w[1118]* flies were crossed with *Act5C-gal4* driver flies. Third-instar larvae were dissected in phosphate-buffered saline (PBS; pH 7.6), and the tracheae were removed and fixed in 4% w/v paraformaldehyde in PBS for 30 min at room temperature. Following blocking with 0.5% bovine serum albumin (BSA) and 0.1% Triton X-100, the tracheae were incubated in a 1:200 dilution of polyclonal

rabbit anti-lysozyme antiserum (Dako UK Ltd., Cambridge, UK) overnight at 4°C, followed by 3 washes and then a 1:1000 dilution of alkaline phosphatase (AP) conjugated anti-rabbit IgG (Promega). We used 5-bromo-4-chloro-3-indonyl-phosphatase in conjugation with nitro blue tetrazolium for colorimetric detection of alkaline phosphatase activity. Samples were examined at ×40 view.

Preparation of lysozyme-specific capture resin

CNBr-activated Sepharose 4B resin (GE Healthcare, Little Chalfont, UK) was suspended in a 1 mM HCl solution (1:10 resin:solution, w/v) for 15 min with gentle agitation. The resin was centrifuged (1100 g, 10 min), and the supernatant was decanted. The resin was then washed 3 times with the HCl solution, and a 2-ml aliquot of resin suspension was centrifuged (2300 g, 2 min), suspended in buffer 1 (0.1 M NaHCO$_3$, pH 8.3, with 0.5 M NaCl), and centrifuged again (2300 g, 2 min). After washing the resin 3 times in this way, it was resuspended in 2 ml of 0.5 mg/ml of cAb-HuL6 (the N-terminal domain of a camelid heavy-chain antibody specific for human lysozyme; ref. 21) dissolved in buffer 1, and incubated overnight with gentle agitation at 4°C. The resin slurry was then centrifuged (2300 g, 2 min), and the supernatant was removed. The resin was successively washed with buffer 1 to remove excess cAb-HuL6 and then incubated in a 1 M ethanolamine solution (1 M, pH 8.0, room temperature, 2.5 h), and washed 3 times with buffer 2 (0.1 M acetate, pH 4, and 0.5 M NaCl) and 3 times with buffer 3 (0.1 M Tris, pH 8, and 0.5 M NaCl). The cAb-HuL6-conjugated resin was finally suspended in buffer 3.

Immunoprecipitation

A 100-μl aliquot of the cAb-HuL6-conjugated resin slurry was placed in a Micro Bio-Spin Chromatography Column (Bio-Rad) and equilibrated by washing the resin 3 times with cold SuperBlock TBS Blocking Buffer (Pierce, Rockford, IL, USA) containing EDTA-free protease inhibitors (TBS-PI; Roche Diagnostics, Burgess Hill, UK). Known numbers of flies (5–50) were homogenized on ice with a pestle in 1.5-ml Eppendorf tubes containing cold TBS-PI (200 μl). The material was then centrifuged (15,700 g, 1 min), and the supernatant was retained and centrifuged a second time, again retaining the supernatant. A positive control was prepared by adding an aliquot of purified WT human lysozyme to the supernatant of the *Drosophila* w^{1118} control line (which does not express human lysozyme). The total protein concentration of the fly supernatant was determined using the DC Protein Assay (Bio-Rad). The fly supernatant was incubated at room temperature for 5 min with cAb-HuL6-conjugated resin equilibrated with TBS-PI. The resin was then centrifuged (1500 g, 1 min) to remove the supernatant and then washed 3 times with cold TBS-PI. To elute the lysozyme from the resin, a urea solution (20 μl: 9 M urea; 1% w/v SDS; 25 mM Tris, pH 6.8; and 1 mM EDTA) was added to the resin, followed by centrifugation (1500 g, 1 min). Samples were analyzed by Western blotting.

Western blot analysis

Samples were separated on 4–12% NuPAGE gels (Invitrogen, Paisley, UK). Proteins were transferred to a 0.2-μm nitrocellulose membrane (Fisher Scientific, Loughborough, UK) in Tris-glycine buffer containing 20% v/v methanol and 0.01% w/v SDS using a Trans-Blot SD semidry electrophoretic transfer cell (15 V constant, 30 min; Bio-Rad Laboratories). The blots were probed with rabbit anti-human lysozyme

polyclonal antiserum (Washington Biotechnology, Columbia, MD, USA) followed by horseradish peroxidise (HRP)-linked anti-rabbit IgG antiserum (New England Biolabs). The blots were developed with the Pierce SuperSignal West Pico kit or Pierce SuperSignal West Femto kit (Perbio Science, Cramlington, UK).

Hemolymph isolation

Hemolymph was isolated from offspring of pUAST WT (WT[b]) and control w^{1118} flies crossed with *Act5C-gal4* (10 flies) and *gmr-gal4* (30 flies) using the protocol described previously (36). In brief, a hole was punctured in the base of an Eppendorf tube with a 22-gauge needle and plugged with cotton wool. This modified tube was placed in a clean Eppendorf tube for hemolymph collection. The heads of the flies were separated from the thorax with a 27-gauge needle, and both parts were placed in the described apparatus and centrifuged (2500 g, 5 min). No liquid was observed in the collection tube at this point, so the fly debris was removed, and a small volume (5 μl) of TBS-PI was added and centrifuged (2500 g, 5 min). After this step, the hemolymph sample was observed in the collection tube; this sample was further diluted 2- and 5-fold in TBS-PI, and the protein concentration of the hemolymph was determined using the Bio-Rad DC Protein Assay. The samples were analyzed by an ELISA specific for human lysozyme. Levels of lysozyme in the hemolymph were normalized to the total soluble protein concentration in the hemolymph.

ELISA analysis

cAb-HuL6 (5 μg/ml in PBS) was adsorbed onto the wells of a 96-well Nunc MaxiSorb microtiter plate (Fisher Scientific) for 1 h at 37°C. The antibody fragment solution was removed, and the plate was washed 6 times with SuperBlock TBS Blocking Buffer. The wells were blocked with BSA (10 mg/ml in TBS) overnight at 4°C. Flies were homogenized in cold TBS-PI, and the samples were centrifuged (15,700 g, 1 min). The supernatant was retained and centrifuged a second time, again retaining the supernatant. A positive control was prepared by adding an aliquot of purified WT lysozyme to the supernatant of the *Drosophila* w^{1118} control line. A standard curve from known lysozyme concentrations was prepared with purified human lysozyme (0.8 to 20 μg/L) produced recombinantly in *P. pastoris* (27) The total protein concentration in each *Drosophila* supernatant solution was determined using the DC protein assay (Bio-Rad). The supernatant samples, either undiluted or diluted (1:10 dilution in TBS), were incubated for 1 h at 37°C in the wells. The wells were then washed 6 times with TBS and incubated with rabbit anti-human lysozyme antiserum (diluted 1:1000 in 10 mg/ml BSA in TBS; Washington Biotechnology) for 1 h at 37°C. The wells were then again washed 6 times with TBS, followed by incubation with an alkaline phosphatase-conjugated anti-rabbit IgG antiserum (diluted 1:2000 in 10 mg/ml BSA in TBS; New England Biolabs) for 1 h at 37°C. The wells were then washed with TBS a further 6 times, and detection was performed with the ELISA amplification kit (Invitrogen), following the manufacturer's instructions. The recombinant cAb-HuL6 capture antibody is specific for human lysozyme and has a similar affinity (K_D ~1 nM) for the WT, F57I, and D67H lysozymes (21). To test for the presence of insoluble lysozyme in the *Drosophila* samples, flies were homogenized in cold TBS-PI and the samples were centrifuged (15700 g, 1 min). As a positive control, an aliquot of preformed lysozyme fibrils was added to the negative control w^{1118} sample prior to homogenization. The supernatant was removed, and the

insoluble pellet was washed with TBS-PI 3 times, followed by incubation in DMSO (50 µl) for 30 min. The samples were centrifuged (15,700 g, 1 min), and the supernatant was removed. The pure DMSO sample was diluted to a final concentration of 16% DMSO in TBS-PI buffer (to ensure that the lysozyme present would bind in the ELISA analysis). A standard curve of known lysozyme concentrations was prepared in the presence of 16% DMSO, and the ELISA analysis was performed as detailed above.

Scanning electron microscopy (SEM) for *Drosophila* eye analysis

pBS WT, F57I, I59T, D67H, and control w^{1118} flies were crossed with the driver *gmr-gal4*. Crosses were performed at 29°C, and the flies were collected on the day of eclosion. Flies were then dried for 1 d at room temperature, followed by coating with Au/Pd in a Polaron E5000 (Quorum/Emitech, Ashford, UK). The external surfaces of the eyes were visualized by SEM, and the architecture of the retina was viewed. Images were collected using an FEI Philips XL30 scanning electron microscope at 5 kV (Philips, Amsterdam, The Netherlands).

Preparation of flies and immunohistochemistry for UPR detection

pBS WT, F57I, I59T, D67H, and control w^{1118} flies were crossed with the driver *gmr-gal4*. Offspring with the genotype *UAS-lysozyme/Cyo;gmr-gal4/TM6B* were then crossed with UAS-xbp1 flies. Flies were maintained at 29°C. *Drosophila* heads were embedded on the day of eclosion in Tissue-Tek OCT compound (Histolab, Göteborg, Sweden) using Cryomold-specimen molds and stored at −80°C until use. The OCT blocks were sectioned using a Microm HM 550 Cryostat (Microm International GmbH, Walldorf, Germany) into 14-µm thin sections that were placed on SuperFrost Plus slides (Menzel-Gläser, Braunschweig, Germany) and stored at −20°C until use. The sections were fixed in 4% w/v PFA for 10 min at room temperature. The slides were washed in PBS (3×3 min) followed by (1×3 min) wash in PBS-T (PBS with 0.05% v/v Tween-20) before blocking in 10% w/v BSA in PBS-T for 1 h at room temperature. Rabbit anti-GFP antibody (1:2000 in 1% BSA w/v in PBS-T; Chemokine, Secaucus, NJ, USA) was added to the slides and incubated overnight at 4°C. The slides were washed with PBS-T (3×5 min). Goat-anti-rabbit fluorescently labeled secondary antibody (1:500 in 1% w/v BSA in PBS-T; Alexa Fluor 594 Goat-anti-Rabbit; Invitrogen) was applied to the slides and incubated for 1 h at room temperature. The slides were washed with PBS-T (3×10 min), dipped in dH$_2$O, and allowed to dry for a couple of minutes in the dark. The slides were mounted using Vectashield with DAPI (Vector Laboratories, Peterborough, UK) and sealed with nail polish. The slides were analyzed using a Leica DM6000 microscope (Leica Microsystems, Wetzlar, Germany) using the 405/40 nm (for DAPI) and 560/40 nm (for Alexa) bandpass filters. Micrographs were processed in Adobe Photoshop CS4 (Adobe Systems, San Jose, CA, USA); background levels were reduced, the signal levels were enhanced, and scale bars were added. All images were treated identically. The GFP-positive cells were quantified in a blinded experiment where 16, 15, 14, 21, and 18 micrographs for control, WT, I59T, D67H, and F57I, respectively, were examined for GFP-positive cells that colocalized with DAPI.

Statistical analysis

Statistical comparisons were performed with a 2-tailed unpaired Student's t test, (GraphPad Prism 5; GraphPad, La Jolla, CA, USA).

RESULTS

WT lysozyme is efficiently secreted into the fly hemolymph

In this study, we have investigated the tissue-directed expression of lysozyme in *Drosophila* using the *UAS-gal4* system (41) and the two drivers *Act5C-gal4* (ubiquitous expression; ref. 42) and *gmr-gal4* (retinal expression; ref. 43). Two different *gal4*-responsive vectors, pUAST and pBS-LoxP-white-Lox2272 (pBS), were used to produce our transgenic models. The important difference between these transgenesis systems is that pUAST inserts pseudorandomly throughout the genome, while the pBS-LoxP vector directs insertion to a unique location in an engineered acceptor site (39, 41). In both cases, the gene for lysozyme was fused to a signal peptide sequence derived from the *Drosophila* protein called necrotic (38), and efficient secretion of the WT protein was observed for both *Act5C-gal4* and *gmr-gal4* (**Fig. 1**). The circulating level of WT lysozyme in the flies was calculated to be ~0.7 mg/L and ~0.2 mg/L when expressed by the *Act5C-gal4* and *gmr-gal4* drivers,
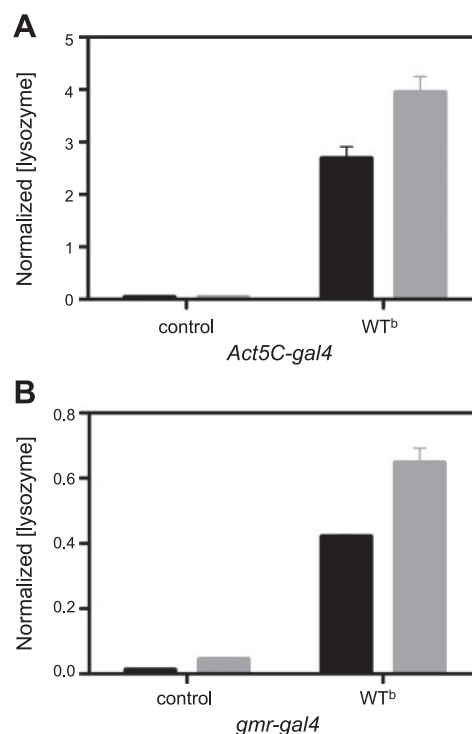
Figure 1. Secreted levels of lysozyme. ELISA analysis of hemolymph isolated from offspring of *Act5C-gal4* (*A*) and *gmr-gal4* driver (*B*) crosses with WT[b] and w^{1118} (control) flies. The analysis clearly shows the presence of human lysozyme in the WT[b] line and its absence in the control flies in both cases. The quantity of lysozyme present in the hemolymph isolates (solid bars) was found to be ~65% of the amount of lysozyme present in the whole fly (shaded bars). Levels of lysozyme in the hemolymph were normalized to the total soluble protein concentration in each hemolymph sample. Normalized (lysozyme) values were calculated as nanograms of lysozyme present per total amount of soluble lysate proteins (mg/ml). Data are means ± SD.
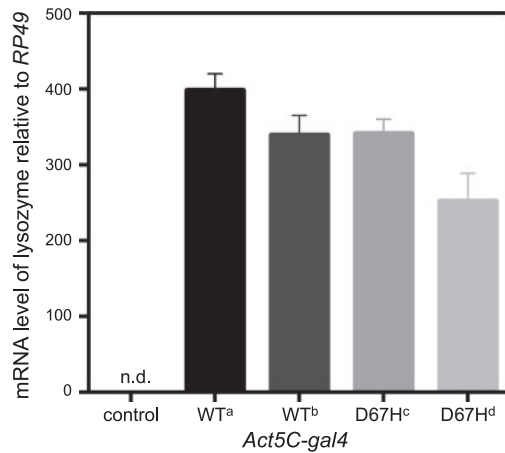
Figure 2. qRT-PCR analysis of lysozyme transcription levels. The levels of lysozyme mRNA in each of two independent lines of WT lysozyme (WT[a] and WT[b]) and of D67H lysozyme (D67H[c] and D67H[d]) and w^{1118} (control) flies were analyzed by qRT-PCR. The lysozyme protein was expressed using the *Act5C-gal4* driver. All values were normalized against the level of the housekeeping gene *RP49* (see Materials and Methods). In this analysis, the WT lysozyme line WT[b] was identified to have the same mRNA expression level (within 1%) as the D67H lysozyme line D67H[c], and the controls revealed no detectable levels of lysozyme (n.d.). Data are means ± SD.

respectively. Interestingly, these values are in agreement with literature reports of WT lysozyme levels in a healthy individual being 0.5–3 mg/L (44). In the first instance, several independent transgenic lines of WT and D67H lysozymes were generated using the pUAST plasmid. The transcriptional levels for each line were analyzed by qRT-PCR to allow selection of WT and D67H lines that expressed lysozyme at equivalent levels. Despite large differences in mRNA levels for the variants, two lines, WT[b] and D67H[c], yielded equivalent mRNA levels for WT and D67H lysozyme, respectively (**Fig. 2**).

High levels of WT lysozyme are lethal during metamorphosis

The qRT-PCR analysis confirmed the presence of transcriptionally active lysozyme transgenes for both WT and D67H-transgenic *Drosophila* lines. Therefore, we investigated the effect of expressing WT and D67H lysozymes ubiquitously in the fly using the driver *Act5C-gal4*. When the WT[b] and D67H[c] transgenes were expressed in this way, we observed partial pupal lethality (*i.e.*, a substantial number of the flies failed to eclose) for WT lysozyme (**Fig. 3B**), but not for the D67H variant (Fig. 3*C*). In addition, a more marked lethality was observed for the WT[a] line, which thus correlates with the higher transcriptional activity obtained for WT[a] compared to WT[b] (Fig. 2). In contrast, all flies expressing the D67H variant developed normally (Fig. 3*C*) as compared to the w^{1118} control flies (Fig. 3*A*). Immunohistochemistry was used to probe for the presence of lysozyme; the WT protein was readily detected in the

tracheae of third instar larvae (Fig. 3*E*), but no staining was observed for D67H[c] or for the control larvae (Fig. 3*F*, *D*, respectively).

WT lysozyme is more abundant than the disease-associated D67H variant

Immunoprecipitation followed by Western blotting of homogenates from whole flies that expressed lysozyme ubiquitously demonstrated the presence of both the WT (**Fig. 4A,** lanes 4 and 5) and the D67H (Fig. 4*A*, lanes 6 and 7) isoforms, with seemingly lower signals for the D67H variant. To quantify this result, a sensitive ELISA assay was developed using the recombinant cAb-HuL6 (the N-terminal domain of a camelid heavy-chain antibody specific for human lysozyme) as the capture antibody and a polyclonal antiserum for detection. From the ELISA results, it was apparent that newly eclosed flies exhibited 5-fold higher levels for the WT protein than for the D67H variant (Fig. 4*B*). These data confirm the results from the immunohistochemistry and Western blot experiments, where, in both cases, higher protein levels were detected for the WT lysozyme than for the D67H variant (Figs. 3*E*, *F* and 4*A*, lanes 4–7, respectively).

Levels of soluble lysozyme correlate with the native-state stability of the protein

To determine whether the soluble levels of lysozyme are related to the native-state stabilities of the proteins, we used the site-directed insertion method of the pBS system to generate 4 transgenic lines expressing the WT
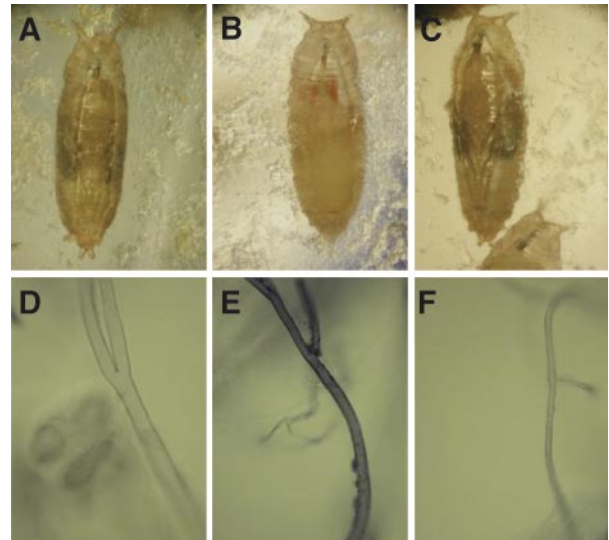

Figure 3. Pupae analysis and immunohistochemistry. *A–C*) Images of larval development during metamorphosis of *Drosophila* expressing no lysozyme (control w^{1118}; *A*), WT lysozyme (WT[b]; *B*), and D67H lysozyme (D67H[c]; *C*). *D–F*) Immunohistochemical analysis of trachea tissue, probed with an anti-lysozyme antibody, of *Drosophila* expressing no lysozyme (*D*), WT lysozyme (*E*), and D67H lysozyme (*F*). The lysozyme protein was expressed using the *Act5C-gal4* driver.
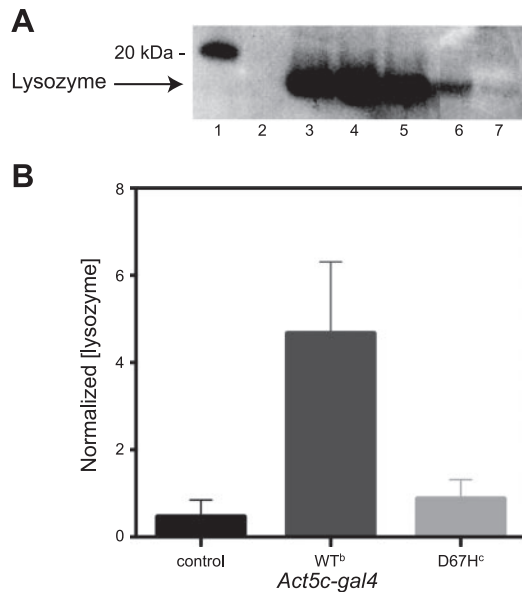
Figure 4. Western blot and ELISA analysis of *Drosophila* lines expressing lysozyme ubiquitously. *A*) Western blot analysis of offspring, collected at d 0, from WT and D67H pUAST lysozyme lines crossed with the *Act5C-gal4* driver (100 flies/sample), which drives expression of lysozyme ubiquitously. Lane 1: markers; lane 2: negative control (w^{1118}); lane 3: positive control (w^{1118} lysate spiked with recombinant human lysozyme); lane 4: WT[a]; lane 5: WT[b]; lane 6: D67H[c]; lane 7: D67H[d]. *B*) ELISA analysis of offspring, collected at d 0, from control, WT[b], and D67H[c] flies that were crossed with the *Act5C-gal4* driver. Normalized (lysozyme) values were calculated as nanograms of lysozyme present per total amount of soluble lysate proteins (mg/ml). Data are means ± SD.

lysozyme; the I59T variant, which has a lower stability compared to the WT protein; and the most destabilized amyloidogenic variants, F57I and D67H (3, 17, 18, 45) at comparable levels. The differences in the native-state stabilities of WT, F57I, I59T, and D67H lysozymes have previously been examined, and the midpoints of thermal denaturation are reported to be 79.2 ± 1.4, 60.4 ± 1.1, 70.1 ± 1.3, and 66.0 ± 2.0°C, respectively (27).

ELISA measurements on flies expressing lysozyme through the *Act5C-gal4* driver revealed that the destabilized F57I and D67H lysozyme variants are present at substantially lower levels than WT lysozyme and that the level of soluble protein in *Drosophila* correlates well with the stability of the lysozyme variants. The level of the I59T variant was found to be 3-fold lower than that of WT but 6-fold higher than that of the amyloidogenic variants (**Fig. 5A**). A similar correlation between the stability of lysozyme and the detected levels of protein was found in flies expressing lysozyme in the fly retina through the *gmr-gal4* driver, where the detected levels of the I59T variant were found to be 4-fold lower than the WT protein but 2- and 3-fold higher than the amyloidogenic variants F57I and D67H, respectively (Fig. 5B). The results from the ELISA measurements are summarized in Supplemental Table S1.

It has been reported that the rates of *in vitro* aggregation of the amyloidogenic variants, as well as the I59T variant, are higher than WT lysozyme (17, 23); there-

fore, to determine whether the lower level of soluble protein was due to the variants being trapped as insoluble aggregates within the flies, an additional extraction step using DMSO (which can completely dissolve fibrils; ref. 46) was added after homogenizing the flies in TBS-PI. The DMSO extracts were isolated and analyzed by ELISA. The results showed that a sample of w^{1118} control flies that had been spiked with preformed lysozyme fibrils prior to homogenization gave a strong positive lysozyme signal in the ELISA assay; however, no significant signal was detected after DMSO solubilization of the lysozyme flies crossed with the *gmr-gal4* driver (Supplemental Fig. S1). This suggests that the lower level of soluble protein is due to degradation of the less stable lysozyme variants and not due to aggregate accumulation.
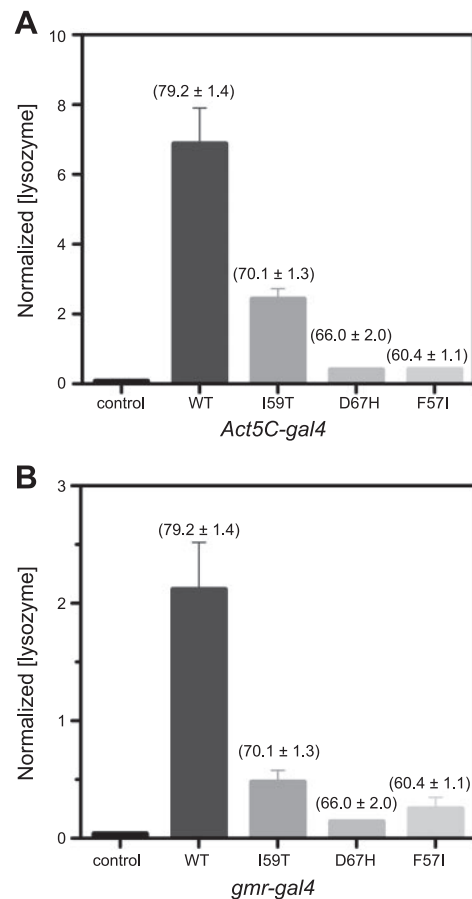

Figure 5. ELISA analysis of *Drosophila* lines expressing lysozyme variants that differ in their native-state stability. ELISA analysis of offspring, collected at d 0, from various pBS lysozyme lines. *A*) Offspring from w^{1118} (control), WT, I59T, D67H, and F57I flies that were crossed with the *Act5C-gal4* driver, which drives expression of lysozyme ubiquitously. *B*) Offspring from control, WT, I59T, D67H, and F57I flies that were crossed with the *gmr-gal4* driver, which drives expression of lysozyme in the retina of *Drosophila* eyes. Normalized (lysozyme) values were calculated as nanograms of lysozyme present per total amount of soluble lysate proteins (mg/ml). Data are means ± SD. Native-state stability of the lysozyme variants is indicated above each bar; these values are based on thermal denaturation, as reported previously (27).

Expression of destabilized lysozyme variants in the retina results in a rough-eye phenotype

Using *gmr-gal4* to drive retinal expression of the WT, F57I, I59T, and D67H lysozymes, a significant rough-eye phenotype was observed for flies expressing F57I lysozyme (**Fig. 6E**). For these flies, the normal regular pattern of the ommatidia, which is observed in the *gmr-gal4* background w^{1118} control flies (Fig. 6A), is highly disrupted, and some of the ommatidia are fused together. In addition, a mild rough-eye phenotype for flies expressing D67H lysozyme could be observed (highlighted by lines in Fig. 6D). This phenotype was not apparent for the *gmr-gal4* background control flies (Fig. 6A) or when WT or I59T lysozyme was expressed in the fly retina (Fig. 6B, C, respectively). These results indicate that the expression of the amyloidogenic lysozyme variants results in significant toxicity during the development of the *Drosophila* eye despite the fact that the major fractions of the proteins are cleared from the system.

Unfolded protein response is triggered by expression of the destabilized lysozyme variants

To investigate whether the rough-eye phenotype could be due to ER stress and the resulting activation of the UPR, xbp1-EGFP was coexpressed with lysozyme in the fly retina using *gmr-gal4*. The marker xbp1-EGFP can be used specifically to detect the Ire-1 pathway of the UPR activation. Splicing of a transgenic xbp1-EGFP-mRNA by Ire-1 brings the EGFP coding sequence into frame, generating a signal that can be detected by a variety of microscopic techniques (47).

The Ire-1-dependent generation of EGFP in horizontal micrographs of the eye of an adult fly was detected using an antibody against GFP followed by a fluorescent secondary antibody. Because of the nuclear localization sequence within xbp1, xbp1-EFGP accumulates in the nuclei and is observed as red dots in the micrographs (**Fig. 7A–E,** arrows). Accumulation of GFP in the cell nuclei (red stain) was confirmed by colocalization with the nuclei-specific stain DAPI (blue stain; Fig. 7F). When expressing xbp1-EGFP in the *gmr-gal4* background of control w^{1118} flies, a low signal can be observed, which reveals a basal level of UPR activation in the fly retina (Fig. 7G). No notable increase in the activation of UPR was observed for WT or I59T when expressed through the *gmr-gal4* driver (Fig. 7G). In contrast, expression of F57I and D67H resulted in a significant increase in the activation of the UPR, as indicated by the higher number of GFP-positive cells appearing in the micrographs (Fig. 7G). Interestingly, these data show that the UPR is activated by the most destabilized amyloidogenic variants, which also display a distinct rough-eye phenotype (Fig. 6D, E).

DISCUSSION

Individual human patients expressing one of the naturally occurring amyloidogenic lysozyme variants (I56T, F57I, W64R, D67H, F57I/T70N, and T70N/W112R) are at risk of amyloid deposition in a range of tissues, including the spleen and kidney (48). The consequent syndrome, termed systemic amyloidosis, is thought to result primarily from the presence of large quantities of insoluble protein aggregates, causing disruptive effects on the organs involved (2, 3). Interestingly, neither the spleen nor the kidney synthesizes significant quantities of lysozyme (49), and therefore the variant proteins must be transported to these sites *via* circulation in the blood. Although there is clinical evidence that patients expressing lysozyme variants have reduced levels of this
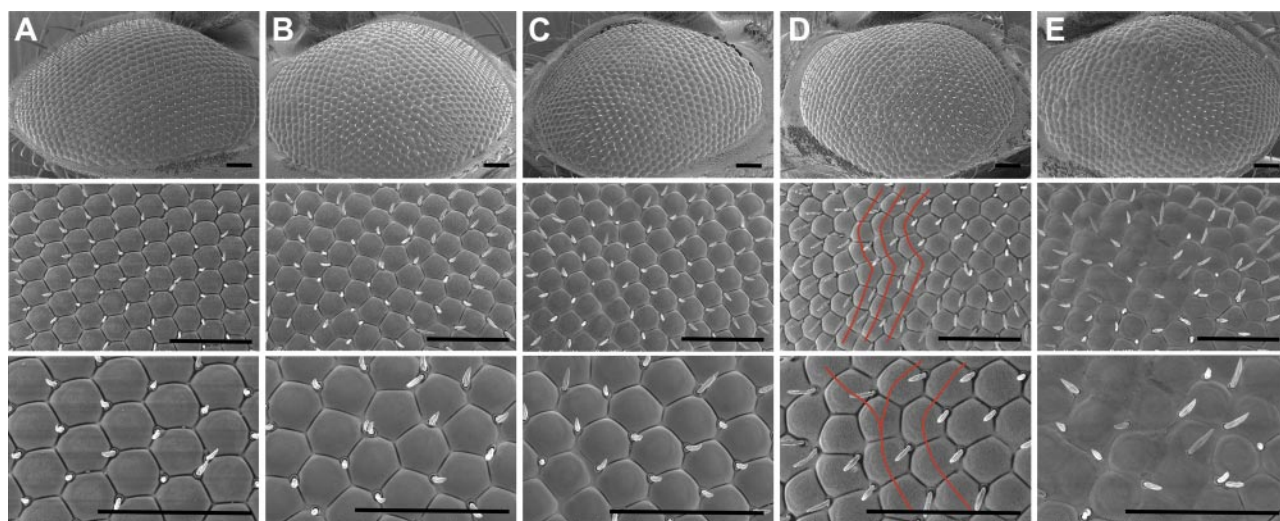

Figure 6. SEM analysis of rough-eye phenotype. Images of *Drosophila* eyes obtained by SEM for *gmr-gal4* background control w^{1118} (*A*), WT (*B*), I59T (*C*), D67H (*D*), and F57I (*E*). A significant disruption in the eye structure was found for the F57I line. The somewhat smaller disruption in the regular pattern of the ommatidia for the D67H line is highlighted by red lines. The lysozyme protein was expressed using the *gmr-gal4* driver. Scale bars = 50 μm.
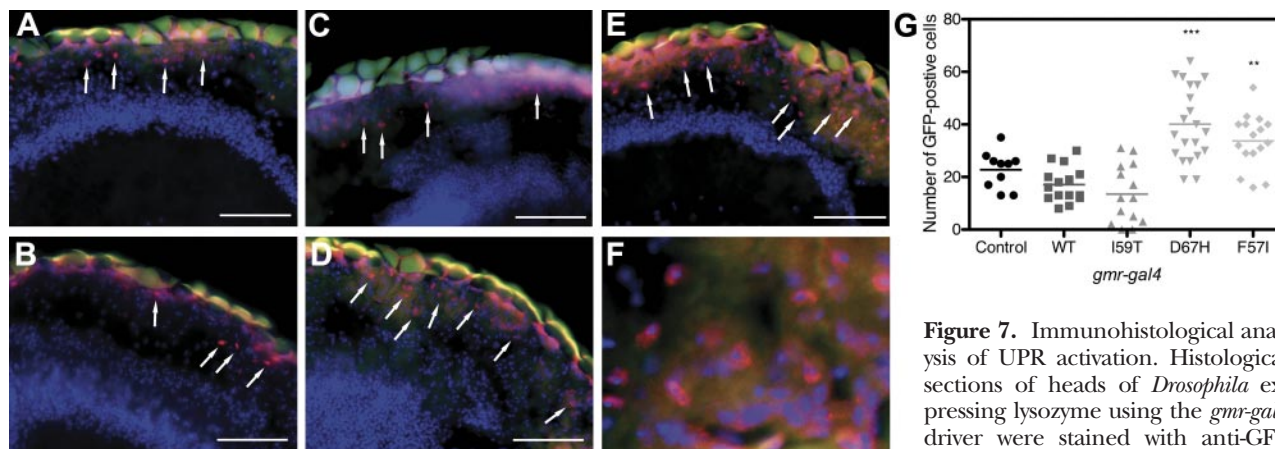
Figure 7. Immunohistological analysis of UPR activation. Histological sections of heads of *Drosophila* expressing lysozyme using the *gmr-gal4* driver were stained with anti-GFP antibody to detect spliced xbp1-EGFP as a marker for IRE1-positive cells, indicating UPR activation (arrows). Red stain shows GFP signal enhanced by Alexa 594-nm secondary antibody. Blue shows staining of cell nuclei by DAPI. A–F) *gmr-gal4* background control w^{1118} (A), WT (B), I59T (C), D67H (D), and F57I (E); accumulation of GFP in the cell nuclei was confirmed by colocalization with DAPI (F). Micrographs were taken at ×40. Scale bars = 50 μm. G) Scatter plot shows number of GFP-positive cells for each variant of lysozyme. Micrographs were examined for GFP-positive cells in a blind experiment. Asterisks indicate significant increase of GFP-positive cells compared to control. **$P < 0.01$, ***$P < 0.001$.

protein in circulation, comprehensive data are not available (4); it appears, however, that despite the patients being heterozygous, only the variant protein has been identified in the amyloid deposits (2).

An important goal of this study was to compare the potentially toxic consequences of the expression of WT and amyloidogenic lysozymes in *Drosophila*. In this respect, the F57I and D67H variants were chosen for our study since the mutations are found naturally, causing hereditary non-neuropathic systemic amyloidosis (2, 5, 49), and the native state of these lysozyme variants is very significantly destabilized relative to the WT protein (18). To explore the relationship between the secreted levels of lysozyme in *Drosophila* and the stability of various lysozyme variants, the non-natural I59T variant was also included in our study since its stability is intermediate between that of the WT protein and the stabilities of the F57I and D67H variants (45).

Gene expression and protein secretion

To ensure that comparisons of the results for the WT and mutational variants are meaningful, we identified transgenes that transcribed the different forms of lysozyme with equal efficiency. This objective was achieved in two ways. First, we generated flies that are transgenic for both the WT and D67H constructs by random genomic insertion and then screened by qRT-PCR for lysozyme mRNA to find pairs of lines that express lysozyme at equal levels. Second, we used site-directed transgenesis to create flies carrying each of the constructs (WT, F57I, I59T, and D67H) at the same genomic location, thus eliminating any effects of different positions of insertion. In this way, we have been able to perform the study using well-matched fly lines expressing the WT and the variant lysozymes.

Analysis of the results from ELISA experiments reveals that in all tissues, the levels of soluble lysozyme for the WT flies are much higher, 5–17 times more abundant, than the protein levels obtained for the F57I and D67H variants. The soluble lysozyme in the I59T flies is at an intermediate level, 3–4 times lower as compared to WT flies but 3–6 times higher with respect to F57I and D67H flies. Thus, there is a clear correlation between the degree of native-state destabilization of each variant and the reduction in the amount of secreted protein. This finding is consistent with previous studies of lysozyme expression in yeast (27) and strongly suggests that the quality control systems of both yeast and *Drosophila* are able to detect and to clear destabilized lysozyme variants.

Lysozyme toxicity during metamorphosis

Interestingly, we found that high levels of ubiquitously expressed WT lysozyme are lethal during metamorphosis, as revealed by the failure of a substantial amount of the pupae expressing the protein to reach maturity and eclose. Lysozyme catalyzes the hydrolysis of glycosidic bonds between *N*-acetylmuramic acid and *N*-acetyl-D-glucosamine residues in peptidoglycans, but it is also capable of degrading chitin, a polysaccharide found in the outer skeleton of insects (50); therefore, although the mechanism of toxicity has not been established, it is likely to be related to the enzymatic activity of the highly abundant WT lysozyme during metamorphosis.

Deleterious effects of lysozyme in the adult fly retina

We have found that expression of the variant F57I lysozyme in the fly retina of the developing eye results in a pronounced disruption of the eye structure. A mild rough-eye phenotype was also detected for retinal expression of D67H but not for the more stable WT or I59T proteins. This observation is remarkable, given

the low level of protein secretion in the adult fly retina, for the F57I and D67H variants relative to WT lysozyme. In contrast to the findings of Aβ aggregates in a *Drosophila* model of Alzheimer's disease that were proposed to cause the observed rough-eye phenotype (30), no accumulation of the lysozyme variants has been detected in our fly model (Supplemental Fig. S1). Consequently, we sought to investigate whether the eye phenotype of F57I and D67H could be a result of stress caused by the presence of misfolded lysozyme in the ER.

Role of the UPR system

UPR is a downstream response to stress in the ER allowing the cell to cope with the overload of unfolded/misfolded proteins (29). By using the xbp1-EGFP reporter to probe the activation of the UPR we were able to demonstrate that the UPR is indeed activated in the neuronal tissue of the fly retina when expressing the disease-associated lysozyme variants F57I and D67H. Moreover, the UPR activation correlates with the eye phenotype as large amounts of EGFP were detected for F57I and D67H, which also show disruption in the eye structure during the development of the *Drosophila* eye. In contrast, expressing WT or I59T in the fly retina does not activate the UPR and does not cause a rough-eye phenotype.

As discussed above, the detectable levels of F57I and D67H are much lower than that of the WT protein despite equal transcriptional levels between F57I, D67H, and WT, confirmed by qRT-PCR (Supplemental Fig. S2). The low stability and, consequently, the high amyloidogenic properties of F57I and D67H compared to WT lysozyme (18) make the F57I and D67H variants less likely to fold correctly in the neurons, resulting in an increase in the quantity of misfolded proteins in the ER. This will cause ER stress and activation of the UPR, which in turn leads to the degradation of the protein by up-regulation of genes that promote ERAD of these unstable variants. In contrast, the highly stable WT protein does not activate the UPR and is therefore not degraded; consequently, a high level of protein is observed in the ELISA measurement. Interestingly, our findings are in close agreement with a recent study, which monitored the up-regulation of genes involved in UPR, ERAD, and ER-phagy in *P. pastoris* expressing different lysozyme variants (28); in both cases, a strong correlation was observed between the decrease in lysozyme native stability and an increase in UPR activation.

Linking UPR activation with disrupted retinal development

Activation of the UPR correlates with the presence of a rough-eye phenotype, since UPR activation is noticeably higher for the F57I and D67H lysozyme variants, which both show a significant eye phenotype compared to WT and I59T, where no such phenotype is apparent.

An important function of the UPR is to maintain protein homeostasis and thus to protect the cells from being overloaded by unfolded or misfolded proteins that eventually would lead to cellular dysfunction and to apoptosis (51, 52). However, if the ER stress is high and prolonged, the UPR will be unable to counteract the accumulation of various unfolded or misfolded proteins, and consequently other pathways may activate the apoptotic process (53).

Activation of Ire-1 up-regulates ERAD and promotes degradation of various ER-localized mRNA molecules. This effect reduces the protein load on the stressed ER and allows reprogramming of ER-associated protein synthesis (29). Notably, in our *Drosophila* system, Ire-1 will constantly be activated by the production of the least stable misfolded lysozyme variants and therefore prevent recovery of protein synthesis in the developing eye. This effect by itself may cause the panel of proteins necessary for correct eye development to be out of balance, resulting in failure of the compound eye to develop normally. Alternatively, or in addition, prolonged activation of Ire-1 in the fly retina during eye development may activate pathways that, in turn, induce cell death (29).

CONCLUSIONS

The delicate balance between the propensity for a misfolded protein to be cleared or to aggregate is a crucial feature that can dictate whether amyloid disease occurs or is avoided. Although the native-state stabilities of the amyloidogenic variants of lysozyme are decreased in thermal stability by ~13–19°C with respect to the WT protein, they are still relatively stable proteins with values of $T_m > 60$°C (27). Nevertheless, our data show that the amyloidogenic variants are sufficiently destabilized to trigger the UPR, resulting in the clearance of a large proportion of the protein; therefore, it would appear that the quality control mechanisms within a healthy organism are quite stringent. In light of our findings, we speculate that the onset of familial amyloid disease may be linked to the inability of the UPR to detect and target for degradation the entire population of the amyloidogenic variants prior to secretion, allowing a proportion of these destabilized species to enter circulation and eventually to aggregate and accumulate in the body as intractable deposits. Thus, enhancing, directly or indirectly, the quality control system for patients with protein misfolding diseases could be beneficial to allow degradation of the misfolded variants, thereby preventing their secretion and eventual aggregation in different organs with fatal outcome.

The fact that the WT and I59T lysozymes exhibit significantly higher levels of secretion compared to F57I and D67H in our *Drosophila* model system will provide an opportunity to screen for potential pharmacological and genetic modifiers of the ER quality control system, using the protein levels of WT and I59T as readouts. The discovery of agents or gene products that

enhance the quality control system, for example, by lowering the secreted level of WT and I59T lysozymes, will constitute potential targets for therapeutic improvement of the quality control system. Also, pharmacological agents and gene products that inhibit aspects of the proteostasis machinery can be screened by the search for products that increase the secreted levels of F57I and D67H.

The *Drosophila* model system presented in this work reveals some of the consequences of UPR activation when lysozyme is overexpressed in the fly. This unique model also provides an initial foundation for generating further insights into the mechanism by which amyloidogenic lysozyme variants are able to evade the quality control system to an extent that the protein can aggregate in patients with these genetic mutations. FJ

REFERENCES

1. Fleming, A. (1922) On a remarkable bacteriolytic element found in tissues and secretions. *Proc. R. Soc. Lond.* **93,** 306–317
2. Pepys, M. B., Hawkins, P. N., Booth, D. R., Vigushin, D. M., Tennent, G. A., Soutar, A. K., Totty, N., Nguyen, O., Blake, C. C. F., Terry, C. J., Feest, T. G., Zalin, A. M., and Hsuan, J. J. (1993) Human lysozyme gene mutations cause hereditary systemic amyloidosis. *Nature* **362,** 553–557
3. Booth, D. R., Sunde, M., Bellotti, V., Robinson, C. V., Hutchinson, W. L., Fraser, P. E., Hawkins, P. N., Dobson, C. M., Radford, S. E., Blake, C. C., and Pepys, M. B. (1997) Instability, unfolding and aggregation of human lysozyme variants underlying amyloid fibrillogenesis. *Nature* **385,** 787–793
4. Valleix, S., Drunat, S., Philit, J. B., Adoue, D., Piette, J. C., Droz, D., MacGregor, B., Canet, D., Delpech, M., and Grateau, G. (2002) Hereditary renal amyloidosis caused by a new variant lysozyme W64R in a French family. *Kidney Int.* **61,** 907–912
5. Yazaki, M., Farrell, S. A., and Benson, M. D. (2003) A novel lysozyme mutation Phe57Ile associated with hereditary renal amyloidosis. *Kidney Int.* **63,** 1652–1657
6. Röcken, C., Becker, K., Fändrich, M., Schroeckh, V., Stix, B., Rath, T., Kähne, T., Dierkes, J., Roessner, A., and Albert, F. W. (2005) ALys amyloidosis caused by compound heterozygosity in exon 2 (Thr70Asn) and Exon 4 (Trp112Arg) of the lysozyme gene. *Hum. Mutat.* **27,** 119–120
7. Hooke, S. D., Radford, S. E., and Dobson, C. M. (1994) The refolding of human lysozyme: a comparison with the structurally homologous hen lysozyme. *Biochemistry* **33,** 5867–5876
8. Hooke, S. D., Eyles, S. J., Miranker, A., Radford, S. E., Robinson, C. V., and Dobson, C. M. (1995) Cooperative elements in protein folding monitored by electrospray ionization mass spectrometry. *J. Am. Chem. Soc.* **117,** 7548–7549
9. Haezebrouck, P., Joniau, M., Van Dael, H., Hooke, S. D., Woodruff, N. D., and Dobson, C. M. (1995) An equilibrium partially folded state of human lysozyme at low pH. *J. Mol. Biol.* **246,** 382–387
10. Canet, D., Sunde, M., Last, A. M., Miranker, A., Spencer, A., Robinson, C. V., and Dobson, C. M. (1999) Mechanistic studies of the folding of human lysozyme and the origin of amyloidogenic behavior in its disease-related variants. *Biochemistry* **38,** 6419–6427
11. Funahashi, J., Takano, K., Ogasahara, K., Yamagata, Y., and Yutani, K. (1996) The structure, stability, and folding process of amyloidogenic mutant human lysozyme. *J. Biochem.* **120,** 1216–1223
12. Takano, K., Funahashi, J., and Yutani, K. (2001) The stability and folding process of amyloidogenic mutant human lysozymes. *Eur. J. Biochem.* **268,** 155–159
13. Canet, D., Last, A. M., Tito, P., Sunde, M., Spencer, A., Archer, D. B., Redfield, C., Robinson, C. V., and Dobson, C. M. (2002) Local cooperativity in the unfolding of an amyloidogenic variant of human lysozyme. *Nat. Struct. Biol.* **9,** 308–315
14. Esposito, G., Garcia, J., Mangione, P., Giorgetti, S., Corazza, A., Viglino, P., Chiti, F., Andreola, A., Dumy, P., Booth, D., Hawkins, P. N., and Bellotti, V. (2003) Structural and folding dynamics properties of T70N variant of human lysozyme. *J. Biol. Chem.* **278,** 25910–25918
15. Johnson, R. J., Christodoulou, J., Dumoulin, M., Caddy, G. L., Alcocer, M. J., Murtagh, G. J., Kumita, J. R., Larsson, G., Robinson, C. V., Archer, D. B., Luisi, B., and Dobson, C. M. (2005) Rationalising lysozyme amyloidosis: insights from the structure and solution dynamics of T70N lysozyme. *J. Mol. Biol.* **352,** 823–836
16. Wain, R., Smith, L. J., and Dobson, C. M. (2005) Oxidative refolding of amyloidogenic variants of human lysozyme. *J. Mol. Biol.* **351,** 662–671
17. Dumoulin, M., Canet, D., Last, A. M., Pardon, E., Archer, D. B., Muyldermans, S., Wyns, L., Matagne, A., Robinson, C. V., Redfield, C., and Dobson, C. M. (2005) Reduced global cooperativity is a common feature underlying the amyloidogenicity of pathogenic lysozyme mutations. *J. Mol. Biol.* **346,** 773–788
18. Dumoulin, M., Kumita, J. R., and Dobson, C. M. (2006) Normal and aberrant biological self-assembly: insights from studies of human lysozyme and its amyloidogenic variants. *Acc. Chem. Res.* **39,** 603–610
19. Morozova-Roche, L. A., Zurdo, J., Spencer, A., Noppe, W., Receveur, V., Archer, D. B., Joniau, M., and Dobson, C. M. (2000) Amyloid fibril formation and seeding by wild-type human lysozyme and its disease-related mutational variants. *J. Struct. Biol.* **130,** 339–351
20. Chamberlain, A. K., Receveur, V., Spencer, A., Redfield, C., and Dobson, C. M. (2001) Characterization of the structure and dynamics of amyloidogenic variants of human lysozyme by NMR spectroscopy. *Protein Sci.* **10,** 2525–2530
21. Dumoulin, M., Last, A. M., Desmyter, A., Decanniere, K., Canet, D., Larsson, G., Spencer, A., Archer, D. B., Sasse, J., Muyldermans, S., Wyns, L., Redfield, C., Matagne, A., Robinson, C. V., and Dobson, C. M. (2003) A camelid antibody fragment inhibits the formation of amyloid fibrils by human lysozyme. *Nature* **424,** 783–788
22. De Felice, F. G., Vieira, M. N., Meirelles, M. N., Morozova-Roche, L. A., Dobson, C. M., and Ferreira, S. T. (2004) Formation of amyloid aggregates from human lysozyme and its disease-associated variants using hydrostatic pressure. *FASEB J.* **18,** 1099–1101
23. Kumita, J. R., Poon, S., Caddy, G. L., Hagan, C. L., Dumoulin, M., Yerbury, J. J., Stewart, E. M., Robinson, C. V., Wilson, M. R., and Dobson, C. M. (2007) The extracellular chaperone clusterin potently inhibits human lysozyme amyloid formation by interacting with prefibrillar species. *J. Mol. Biol.* **369,** 157–167
24. Chan, P.-H., Pardon, E., Menzer, L., DeGenst, E., Kumita, J. R., Christodoulou, J., Saerens, D., Brans, A., Bouillenne, F., Archer, D. B., Robinson, C. V., Muyldermans, S., Matagne, A., Redfield, C., Wyns, L., Dobson, C. M., and Dumoulin, M. (2008) Engineering a camelid antibody fragment that binds to the active site of human lysozyme and inhibits its conversion into amyloid fibrils. *Biochemistry* **47,** 11041–11054
25. Frare, E., Mossuto, M. F., de Laureto, P. P., Tolin, S., Menzer, L., Dumoulin, M., Dobson, C. M., and Fontana, A. (2009) Charac-

terization of oligomeric species on the aggregation pathway of human lysozyme. *J. Mol. Biol.* **387,** 17–27

26. Yerbury, J. J., Kumita, J. R., Meehan, S., Dobson, C. M., and Wilson, M. R. (2009) Alpha2-macroglobulin and haptoglobin suppress amyloid formation by interacting with prefibrillar protein species. *J. Biol. Chem.* **284,** 4246–4254

27. Kumita, J. R., Johnson, R. J. K., Alcocer, M. J. C., Dumoulin, M., Holmqvist, F., McCammon, M. G., Robinson, C. V., Archer, D. B., and Dobson, C. M. (2006) Impact of the native-state stability of human lysozyme variants on protein secretion by *Pichia pastoris. FEBS J.* **273,** 711–720

28. Whyteside, G., Alcocer, M. J., Kumita, J. R., Dobson, C. M., Lazarou, M., Pleass, R. J., and Archer, D. B. (2011) Native-State stability determines the extent of degradation relative to secretion of protein variants from *Pichia pastoris. PLoS ONE* **6,** e22692

29. Ron, D., and Walter, P. (2007) Signal integration in the endoplasmic reticulum unfolded protein response. *Nat. Rev. Mol. Cell. Biol.* **8,** 519–529

30. Crowther, D. C., Kinghorn, K. J., Miranda, E., Page, R., Curry, J. A., Duthie, F. A. I., Gubb, D. C., and Lomas, D. A. (2005) Intraneuronal Aβ, non-amyloid aggregates and neurodegeneration in a *Drosophila* model of Alzheimer's disease. *Neuroscience* **132,** 123–135

31. Finelli, A., Kelkar, A., Song, H. J., Yang, H., and Konsolaki, M. (2004) A model for studying Alzheimer's Abeta42-induced toxicity in *Drosophila melanogaster. Mol. Cell. Neurosci.* **26,** 365–375

32. Iijima, K., Liu, H. P., Chiang, A. S., Hearn, S. A., Konsolaki, M., and Zhong, Y. (2004) Dissecting the pathological effects of human Abeta40 and Abeta42 in *Drosophila*: a potential model for Alzheimer's disease. *Proc. Natl. Acad. Sci. U. S. A.* **101,** 6623–6628

33. Jackson, G. R., Salecker, I., Dong, X., Yao, X., Arnheim, N., Faber, P. W., MacDonald, M. E., and Zipursky, S. L. (1998) Polyglutamine-expanded human huntingtin transgenes induce degeneration of *Drosophila* photoreceptor neurons. *Neuron* **21,** 633–642

34. Warrick, J. M., Paulson, H. L., Gray-Board, G. L., Bui, Q. T., Fischbeck, K. H., Pittman, R. N., and Bonini, N. M. (1998) Expanded polyglutamine protein forms nuclear inclusions and causes neural degeneration in *Drosophila. Cell* **93,** 939–949

35. Marsh, J. L., Walker, H., Theisen, H., Zhu, Y. Z., Fielder, T., Purcell, J., and Thompson, L. M. (2000) Expanded polyglutamine peptides alone are intrinsically cytotoxic and cause neurodegeneration in *Drosophila. Hum. Mol. Genet.* **9,** 13–25

36. Pokrzywa, M., Dacklin, I., Hultmark, D., and Lundgren, E. (2007) Misfolded transthyretin causes behavioral changes in a *Drosophila* model for transthyretin-associated amyloidosis. *Eur. J. Neurosci.* **26,** 913–924

37. Berg, I., Thor, S., and Hammarstrom, P. (2009) Modeling familial amyloidotic polyneuropathy (Transthyretin V30M) in *Drosophila melanogaster. Neurodegener. Dis.* **6,** 127–138

38. Green, C., Levashina, E., McKimmie, C., Daffron, T., Reichhart, J.-M., and Gubb, D. (2000) The *necrotic* gene in *Drosophila* corresponds to one of a cluster of three serpin transcripts mapping at 43A1.2. *Genetics* **156,** 1117–1127

39. Oberstein, A., Pare, A., Kaplan, L., and Small, S. (2005) Site-specific transgenesis by Cre-mediated recombination in *Drosophila. Nat. Methods* **2,** 583–585

40. Livak, K. J., and Schmittgen, T. D. (2001) Analysis of relative gene expression data using real-time quantitative PCR and the 2(-delta delta C(T)) method. *Methods* **25,** 402–408

41. Brand, A. H., and Perrimon, N. (1993) Targeted gene expression as a means of altering cell fates and generating dominant phenotypes. *Development* **118,** 401–415

42. Fyrberg, E. A., Mahaffey, J. W., Bond, B. J., and Davidson, N. (1983) Transcripts of the six *Drosophila* actin genes accumulate in a stage- and tissue-specific manner. *Cell* **33,** 115–123

43. Moses, K., Ellis, M. C., and Rubin, G. M. (1989) The *glass* gene encodes a zinc-finger protein required by *Drosophila* photoreceptor cells. *Nature* **340,** 531–536

44. Porstmann, B., Jung, K., Schmechta, H., Evers, U., Pergande, M., Porstmann, T., Kramm, H. J., and Krause, H. (1989) Measurement of lysozyme in human body fluids: comparison of various enzyme immunoassay techniques and their diagnostic application. *Clin. Biochem.* **22,** 349–355

45. Hagan, C. L., Johnson, R. J., Dhulesia, A., Dumoulin, M., Dumont, J., De Genst, E., Christodoulou, J., Robinson, C. V., Dobson, C. M., and Kumita, J. R. (2010) A non-natural variant of human lysozyme (I59T) mimics the *in vitro* behaviour of the I56T variant that is responsible for a form of familial amyloidosis. *Protein Eng. Des. Sel.* **23,** 499–506

46. Hirota-Nakaoka, N., Hasegawa, K., Naiki, H., and Goto, Y. J. (2003) Dissolution of beta2-microglobulin amyloid fibrils by dimethylsulfoxide. *J. Biochem.* **134,** 159–164

47. Ryoo, H. D., Domingos, P. M., Kang, M. J., and Steller, H. (2007) Unfolded protein response in a *Drosophila* model for retinal degeneration. *EMBO J.* **26,** 242–252

48. Pepys, M. B. (2006) *Amyloidosis Ann. Rev. Med.* **57,** 223–241

49. Gillmore, J. D., Booth, D. R., Madhoo, S., Pepys, M. B., and Hawkins, P. N. (1999) Hereditary renal amyloidosis associated with variant lysozyme in a large English family. *Nephrol. Dial. Transplant.* **14,** 2639–2644

50. Lee, Y. C., and Yang, D. (2002) Determination of lysozyme activities in a microplate format. *Anal. Biochem.* **310,** 223–224

51. Cullinan, S. B., and Diehl, J. A. (2004) PERK-dependent activation of Nrf2 contributes to redox homeostasis and cell survival following endoplasmic reticulum stress. *J. Biol. Chem.* **279,** 20108–20117

52. Marciniak, S. J., and Ron, D. (2006) Endoplasmic reticulum stress signaling in disease. *Physiol. Rev.* **86,** 1133–1149

53. Szegezdi, E., Logue, S. E., Gorman, A. M., and Samali, A. (2006) Mediators of endoplasmic reticulum stress-induced apoptosis. *EMBO Rep.* **7,** 880–885